European Journal of Radiology 119 (2019) 108633

Contents lists available at ScienceDirect

European Journal of Radiology

journal homepage: www.elsevier.com/locate/ejrad

Enhancement pattern of hepatocellular adenoma (HCA) on MR imaging performed with Gd-EOB-DTPA versus other Gd-based contrast agents (GBCAs): An intraindividual comparison

Roberto Cannella[a,b], Giuseppe Brancatelli[b], Balasubramanya Rangaswamy[a], Marta I. Minervini[c], Amir A. Borhani[a], Alessandro Furlan[a,*]

[a] Abdominal Imaging Division, Department of Radiology, University of Pittsburgh, 200 Lothrop Street, Pittsburgh, PA, 15213, USA
[b] Section of Radiology - BiND., University Hospital "Paolo Giaccone", Via del Vespro 129, 90127, Palermo, Italy
[c] Division of Transplant Pathology, Department of Pathology, UPMC Montefiore, University of Pittsburgh, PA, United States

ARTICLE INFO

Keywords:
Liver
Hepatocellular adenoma
Magnetic resonance imaging
Contrast media

ABSTRACT

Purpose: To conduct an intraindividual comparison of the enhancement pattern of hepatocellular adenoma (HCA) on dynamic MRI study obtained following the injection of Gadoxetic acid (Gd-EOB-DTPA) and other gadolinium-based contrast agents (GBCAs).

Method: This is a retrospective, Institutional Review Board-approved study conducted in a single institution. A search of medical records between 2008 and 2017 revealed 17 patients (all females) with at least one pathologically-proven HCA who underwent liver MRI with Gd-EOB-DTPA and another GBCA within 1 year. Enhancement of each lesion on hepatic arterial (HAP), portal venous (PVP), 2 min and 4–5 minutes phases was subjectively evaluated by two abdominal radiologists. Lesions were categorized as hyper-, iso- or hypointense compared to the surrounding liver parenchyma. The presence of a peripheral pseudocapsule was also recorded. The differences in lesion enhancement were assessed using the McNemar Test. A p-value < 0.05 was considered statistically significant.

Results: The final population included 35 HCAs (83% inflammatory subtype). There was no significant difference in lesion size ($P = 0.708$) and enhancement on HAP ($P = 0.625$) or PVP ($P = 0.125$). HCAs showed more frequently hypointensity on 2 min (13/35 vs. 1/35, $P < 0.001$) and 4–5 minutes ($P < 0.001$) images obtained after injection of Gd-EOB-DTPA compared to those obtained after other GBCAs. A pseudocapsule was more frequently noted after administration of Gd-EOB-DTPA (13/35 vs 1/35, $P = 0.002$).

Conclusions: Enhancement pattern of HCA differs significantly after the injection of Gd-EOB-DTPA compared to other GBCAs. Lesion hypointensity on 2 min and 4–5 minutes images is more frequent when using Gd-EOB-DTPA.

1. Introduction

Contrast-enhanced magnetic resonance imaging (MRI) is the most informative imaging modality for the diagnosis of hepatocellular adenoma (HCA) [1]. When the diagnosis of HCA is suspected, a hepatobiliary contrast agent such as Gadoxetic acid (Gd-EOB-DTPA) is often the first choice among the available Gadolinium-based contrast agents (GBCAs) because of the reported high accuracy of the hypointensity on hepatobiliary phase (HBP) images in differentiating HCA from focal nodular hyperplasia (FNH) [2,3]. HCA is not a single entity [4,5]. Each molecular subtype carries a different risk of complications (i.e. hemorrhage and malignant transformation) [6,7] and may be identified based on key imaging features, including the enhancement pattern on contrast-enhanced MR images [1,8–11].

Several authors have reported different imaging findings on the post-contrast dynamic studies for hepatocellular carcinoma (HCC)

Abbreviations: APHE, arterial phase hyperenhancement; FNH, focal nodular hyperplasia; GBCAs, gadolinium-based contrast agents; Gd-BOPTA, Gadobenate Dimeglumine; Gd-BT-DO3A, gadobutrol; Gd-DTPA, Gadopentetate Dimeglumine; Gd-DTPA-BMA, gadodiamide; Gd-EOB-DTPA, gadoxetic acid; HAP, hepatic arterial phase; HBP, hepatobiliary phase; HCA, hepatocellular adenoma; HCC, hepatocellular carcinoma; MRI, magnetic resonance imaging; PVP, portal venous phase; TP, transitional phase

* Corresponding author at: 200 Lothrop Street, 15213, Pittsburgh, PA, USA.
E-mail address: furlana@upmc.edu (A. Furlan).

https://doi.org/10.1016/j.ejrad.2019.08.002
Received 31 January 2019; Received in revised form 20 July 2019; Accepted 5 August 2019

[12–14], hepatic hemangioma [15] and FNH [16] following the injection of a purely or predominantly extracellular GBCAs or Gd-EOB-DTPA. The observed dissimilarities have been attributed to the different pharmacokinetics properties of these contrast agents. We hypothesize that the post-contrast MRI appearance of HCA might also differ depending on the type of contrast agent used. Although the imaging appearance of HCA on contrast-enhanced MRI has been extensively investigated [8–11,17–23], the literature evaluating HCA with both Gd-EOB-DTPA and other GBCAs is scant [24,25] and, to the best of our knowledge, such comparison has not yet been reported for dynamic imaging.

The purpose of our study was to conduct an intraindividual comparison of enhancement pattern of HCA on contrast-enhanced MR imaging obtained after the injection of Gd-EOB-DTPA versus other GBCAs.

2. Material and methods

The institutional review board approved this HIPAA-compliant retrospective study. The requirement for informed consent was waived.

2.1. Study population

A search through the medical and pathological records between January 2008 and December 2017 was conducted to identify patients matching the following inclusion criteria: i) age ≥ 18 years; ii) at least one pathologically proven HCA; iii) available Gd-EOB-DTPA MR imaging performed 6 months within the histological analysis and immunohistochemical classification. We identified 51 consecutive patients (50 females, 1 male) matching the inclusion criteria. Among them, 20 (39%) patients (all females) also had a liver MRI with a different GBCA performed within one year of the Gd-EOB-DTPA enhanced MRI. Three patients were excluded because of: *i)* interval appearance of macroscopic intralesional hemorrhage between the two imaging studies (n = 1); *ii)* lack of adequate quality arterial phase imaging (Gd-BOPTA, n = 1); *iii)* resection of the lesion between the two imaging studies (n = 1). The final population consisted of 17 patients (all females, mean ± SD age, 37 ± 11 years; range, 24–62 years).

2.2. MR imaging technique

The MRI studies were performed on 1.5 T or 3 T MR scanners (General Electric, Healthcare, Milwaukee, WI, USA and Siemens Healthcare, Erlangen, Germany). Six of thirty-four (17%) MRI studies were performed at an outside institution and loaded into our system for review and patient's management. For the Gd-EOB-DTPA enhanced MRI, patients received an intravenous administration of 0.025 mmol/Kg or maximum 10 ml of Gd-EOB-DTPA (Gadoxetic acid, Eovist, Bayer Healthcare Pharmaceuticals, Whippany, NJ) with injection rate of 1 mL/sec or 2 mL/sec. In 14 patients, the MRI study performed with other GBCAs was obtained with the intravenous administration of 0.1 mmol/Kg (maximum 24 ml) of Gd-BOPTA (Gadobenate Dimeglumine, MultiHance, Bracco Diagnostics, Princeton, NJ) with injection rate of 2 mL/sec. In our Institution, Gd-BOPTA is used as an extracellular contrast agent since HBP images are not acquired. The remaining three patients were imaged with a purely extracellular agent, including: n = 1, Gd-DTPA (Gadopentetate Dimeglumine. Magnevist, Bayer HealthCare Pharmaceuticals, Whippany, NJ); n = 1 Gd-DTPA-BMA (Gadodiamide, Omniscan, GE Healthcare, Milwaukee, WI) and n = 1 Gd-BT-DO3A (Gadobutrol, Gadavist, Bayer HealthCare Pharmaceuticals, Whippany, NJ) at the dose rate of 0.1 mmol/Kg. The dynamic study consisted of axial T1-weighted three-dimensional (3D) GRE with fat suppression (Liver Acquisition with Volume Acceleration, LAVA or Volumetric Interpolated Breath-hold Examination, VIBE) obtained before and after contrast administration with the following parameters: slice thickness, 4.0–5.0 mm; TR, 3.92–7.14 ms; TE, 1.89–3.12 ms; FA, 12°. Images were obtained during the following post-contrast phases: hepatic arterial phase (HAP), single acquisition with delay of 25–35 seconds (obtained with either test-bolus or fluoroscopic-triggering technique); portal venous phase (PVP), delay of 60–70 seconds; and two additional phases obtained at 2 min and 4–5 minutes post contrast injection. The images obtained at 2 min and 4–5 minutes post injection of Gd-EOB-DTPA are referred to as "transitional" phase (TP) [26]. For Gd-EOB-DTPA enhanced MRI, additional axial images were obtained during the HBP with approximately 20 min delay following contrast injection. No HBP images were obtained after injection of Gd-BOPTA. The interval time between the two MR imaging studies was 192 ± 86 days (range 5–263 days). The Gd-EOB-DTPA enhanced MRI was performed as first examination in nine (53%) patients.

2.3. Imaging analysis

The study coordinator identified the index lesions for analysis and measured the lesion size (maximum diameter) on the axial post-contrast phase better showing the lesion margins. When there were multiple HCAs, the path-proven lesions and those showing identical MR imaging presentation were included with a maximum of three lesions per patient. Lesions with the same MR imaging appearance (i.e. signal intensity on T1-weighted and T2-weighted imaging and post-contrast enhancement pattern) were considered as of the same molecular subtype as the pathologically proven lesion. The image analysis was performed independently by two abdominal radiologists (R.C. and A.F.). To avoid recall bias, MRI studies with Gd-EOB-DTPA and those with other GBCAs were reviewed in two different section two weeks apart. In case of disagreement the images were reviewed and analyzed in consensus. The readers were blinded to the molecular subtype classification of HCAs.

Enhancement of HCAs compared to the surrounding liver parenchyma was evaluated qualitatively and recorded on each post-contrast phase. Arterial phase hyperenhancement (APHE) was considered moderate-to-marked when the lesion showed enhancement similar to or higher than the portal vein on HAP images and mild when the enhancement was less than the portal vein. Lesion hypointensity on PVP, 2 min and 4–5 minutes phases was noted when the signal intensity of the whole or part of the lesion was less than the surrounding parenchyma. In addition, the readers recorded the presence or absence of a lesional "pseudocapsule" defined as a thin peripheral continuous rim with signal intensity different from lesion and the surrounding parenchyma on post-contrast images [8,9,27]. The readers also recorded the signal intensity of the lesion on the HBP images obtained after administration of Gd-EOB-DTPA as hypointense, isointense or hyperintense.

2.4. Statistical analysis

The significance of the difference in lesion enhancement on each post-contrast phase between the two MRI studies was assessed using the McNemar Test. The difference in the size of the lesions between the two MRI studies was calculated using the paired t-test. A p-value < 0.05 was considered statistically significant. Statistical analysis was conducted using SPSS software (version 18.0; SPSS, Chicago, Ill) and MedCalc for Windows (version 17.1, Ostend, Belgium).

3. Results

Thirty-five HCAs in 17 patients were included in the final population, classified as: inflammatory (n = 29, 83%), HNF1α-mutated (n = 2, 6%), β-catenin-mutated (n = 1, 3%), and unclassified (n = 3, 8%) HCAs. Eight patients had a single lesion, while 9 patients had multiple lesions (mean, 15 lesions; range, 4–30 lesions). Pathologic confirmation was available for 20/35 (57%) lesions (percutaneous needle biopsy, n = 16; surgical resection, n = 4). The remaining 15/35

Table 1
Enhancement pattern of HCAs (n = 35) on MR images obtained with Gd-EOB-DTPA and other Gadolinium-based contrast agents (GBCAs).

	Gd-EOB-DTPA	Other GBCAs	P
Moderate-to-marked APHE			0.625
Present	33 (94)	31 (89)	
Absent	2 (6)	4 (11)	
Hypointensity on PVP			0.125
Present	5 (14)	1 (3)	
Absent	30 (86)	34 (97)	
Hypointensity on 2 minutes phase			< 0.001*
Present	13 (37)	1 (3)	
Absent	22 (63)	34 (97)	
Hypointensity on 4-5 minutes phase			
Present	30 (86)	1 (3)	< 0.001*
Absent	5 (14)	34 (97)	
Pseudocapsule			0.002*
Present	13 (37)	1 (3)	
Absent	22 (63)	34 (97)	

Numbers in parentheses are percentages. APHE: arterial phase hyperenhancement; PVP: portal venous phase. GBCAs: Gadolinium-based contrast agents. *: statistically significant: P < 0.05.

(43%) lesions were classified based on similar imaging appearance to the pathologically-proven lesion. Size of the lesions measured on the Gd-EOB-DTPA enhanced MR images (mean, 2.9 ± 2.0 cm; range, 1.0–10.7 cm) was not significantly different from what measured on the MR images obtained with other GBCAs (mean, 2.9 ± 1.9 cm; range, 0.9–10.7 cm; P = 0.708).

The results of image analysis are summarized in Table 1. The number of HCAs showing moderate-to-marked APHE after injection of Gd-EOB-DTPA and other GBCAs was not significantly different (33/35, 94% vs 31/35, 89% - P = 0.625). Five out of 35 (14%) HCAs appeared hypointense on the PVP images obtained after injection of Gd-EOB-DTPA while only one (3%) HCA was hypointense on PVP images obtained after other GBCAs (P = 0.125). Lesion hypointensity was more frequently detected on 2 min (13/35, 37% vs. 1/35, 3% - P < 0.001) and 4–5 minutes (30/35, 86% vs. 1/35, 3% - P < 0.001) images obtained after Gd-EOB-DTPA compared to those obtained after other GBCAs (Fig. 1). Three out of 5 lesions (9% of all HCAs) lacking hypointensity on 4–5 minutes Gd-EOB-DTPA enhanced images were also iso- (n = 1) or hyperintense (n = 2) on the HBP images and were classified as inflammatory (n = 2) or β-catenin mutated (n = 1) HCAs. The remaining 32/35 (91%) HCAs were hypointense on the HBP images acquired after the injection of Gd-EOB-DTPA. A peripheral pseudocapsule was more frequently visualized after the administration of Gd-EOB-DTPA than after the administration of other GBCAs (13/35, 37%, vs 1/35, 3% - P = 0.002) (Fig. 2). The 13 lesions showing pseudocapsule on Gd-EOB-DTPA enhanced MRI were either inflammatory (n = 12) or unclassified (n = 1) HCAs.

Among the inflammatory HCAs (n = 29) lesion hypointensity was observed in 2/29 (7%), 10/29 (34%) and 27/29 (93%) of cases respectively on PVP, 2 min and 4–5 minutes images obtained with Gd-EOB-DTPA while none of the lesions demonstrated hypointensity on the corresponding images obtained with other GBCAs (Figs. 3 and 4). On the HAP images, 27/29 (93%) inflammatory HCAs showed moderate-to-marked APHE after injection of Gd-EOB-DTPA compared to 25/29 (86%) after injection of other GBCAs. The combination of moderate-to-marked APHE and iso- or hyperintensity on PVP and 2 min images would allow the correct classification of inflammatory HCA in 17/29 (58.6%) cases using Gd-EOB-DTPA and 25/29 (86.2%) cases using other GBCAs (P = 0.037).

One of the two HNF1α-mutated (n = 2) HCAs in our population appeared as hypointense on PVP, 2 min and 4–5 minutes images obtained after injection of Gd-EOB-DTPA and Gd-BOPTA. The β-catenin-mutated HCA showed lack of hypointensity on PVP, 2 min and 4–5 minutes images obtained after injection of Gd-EOB-DTPA and Gd-BOPTA.

4. Discussion

In this study we performed an intraindividual comparison of the enhancement pattern of HCA on dynamic MRI study obtained following the injection of Gd-EOB-DTPA and other GBCAs in 17 patients with 35

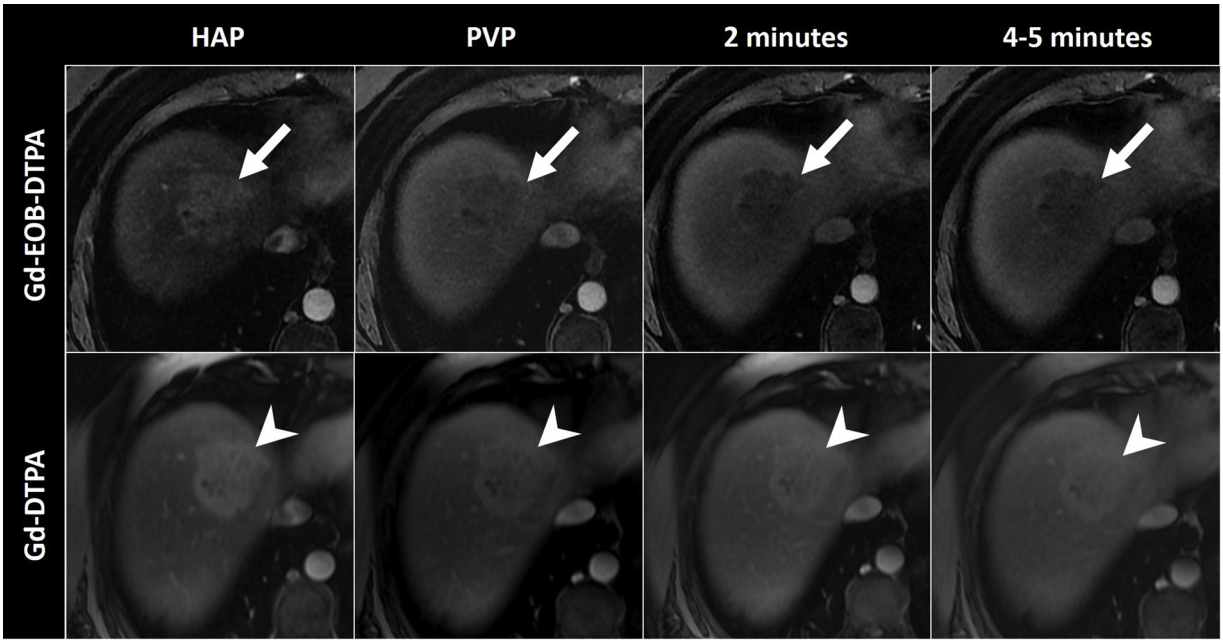

Fig. 1. 43-year-old female with HCA, unclassified subtype, on axial 3D GRE MR images obtained after IV injection of Gd-EOB-DPTA (upper row) and Gd-DTPA (lower row). On Gd-EOB-DTPA enhanced MRI the lesion (*arrows* on upper row) shows marked arterial phase hyperenhancement (APHE) on hepatic arterial phase (HAP) image and hypointensity on portal venous phase (PVP), 2 min and 4–5 minutes phase images. On Gd-DTPA enhanced MRI the lesion (*arrowheads* on lower row) demonstrates marked APHE on HAP image and persistent enhancement on PVP, 2 and 4–5 minutes phase images.

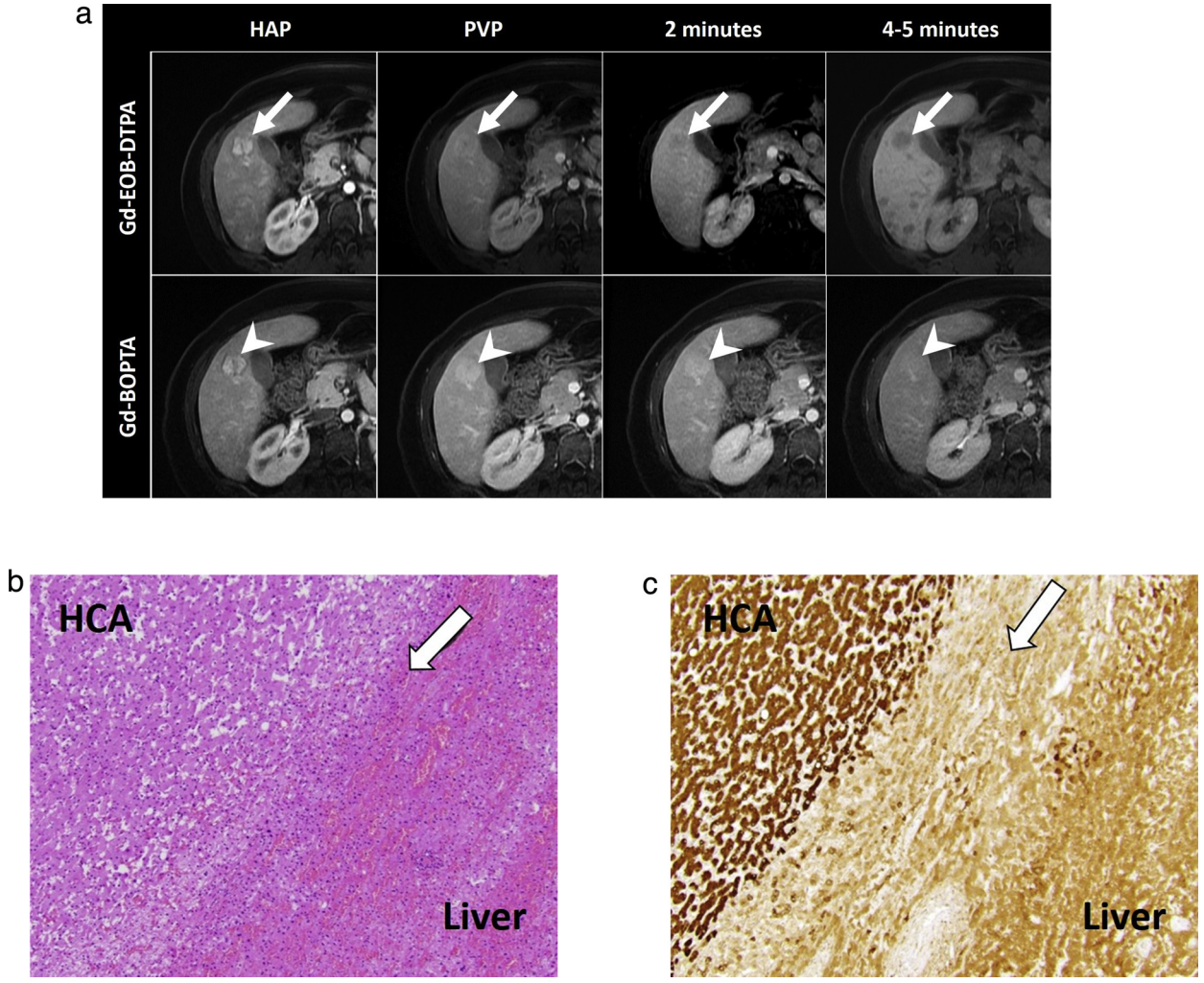

Fig. 2. 46-year-old female with HCA, inflammatory subtype, (**A**) on axial 3D GRE MR images obtained after IV injection of Gd-EOB-DPTA (upper row) and Gd-BOPTA (lower row). On Gd-EOB-DTPA enhanced MRI the lesion (*arrows* on upper row) shows marked APHE on HAP image, isointensity on PVP, hypointensity on 2 min and 4–5 minutes phase images. A peripheral rim of hyperintensity is observed on PVP, 2 and 4–5 minutes phase images. On Gd-BOPTA enhanced MRI the lesion (*arrowheads* on lower row) demonstrates marked APHE on HAP image and persistent enhancement on PVP, 2 and 4–5 minutes phase images. (**B and C**) Hematoxylin and eosin and immunohistochemical stain with lesional positive CRP (C-reactive protein) seen in the resected specimen of the same lesion showing compressed liver parenchyma (arrows) at the interface lesional/non-lesional zone, corresponding to the "pseudocapsule" on the Gd-EOB-DTPA enhanced images.

hepatocellular adenomas. Of note, all patients had at least one pathologically-proven lesion, with immunohistochemical and molecular subclassification. Moreover, a relatively short MRI interval with stable size of the HCAs ensured no significant intra-lesional variability. The main results of our study consist in a larger number of HCAs appearing as hypointense on PVP (14% vs. 3%), 2 min (37% vs. 3%) and 4–5 minutes (86% vs 3%) images obtained after the injection of Gd-EOB-DTPA compared to the corresponding images using other GBCAs. The different enhancement pattern is felt to be due to the inability of the hepatocytes within the lesion to uptake Gd-EOB-DTPA while the contrast is being accumulated into the nontumoral hepatocytes, resulting in higher signal intensity of the background hepatic parenchyma and relative hypointensity of the HCAs. It has been reported that contrast uptake in normally functioning hepatocytes starts at approximately 90 s following IV administration of Gd-EOB-DTPA [26], with a peak at 20 min during the HBP [28]. Our results however suggest that contrast uptake into the hepatocytes may already manifest during the PVP, given the larger number of HCAs appearing hypointense on this phase compared to the corresponding images obtained after injection of a purely or mainly extracellular GBCA. Further studies are necessary to test this hypothesis. If this proves to be true, there might be significant clinical implications when using Gd-EOB-DPTA, not only for imaging hepatic adenomas. The current study, to the best of our knowledge, is the first intraindividual comparison of enhancement pattern of HCAs during the dynamic study obtained with two different GBCAs. Thomeer et al. [24] and Vanhooymissen et al. [25] compared the MR imaging appearance of HCA (21 and 67 lesions, respectively) using Gd-EOB-DTPA and Gd-BOPTA, but their studies were focused on the lesion signal intensity on HBP images.

The results of our study are relevant when using MRI to classify HCAs. Four main molecular subtypes of HCA have been described: HNF1α-mutated, inflammatory, β-catenin mutated and unclassified HCAs [4,5]. Identification of the molecular subtype has significant clinical implications because of the higher reported risk of rupture, hemorrhage (15–20%) and malignant transformation (4.2%) associated with the inflammatory and β-catenin mutated type [29–31]. In this context, the evaluation of the dynamic study after administration of an extracellular contrast agent is key to classify the inflammatory subtype usually manifesting as markedly enhancing lesion on HAP images with persistent enhancement on PVP and delayed phases images, reflecting the presence of dilated vascular spaces (i.e. telangiectasia or sinusoidal dilatation) within the lesion [1,32,33]. The lack of hypointensity (i.e. persistent enhancement) on PVP and delayed phase images is a key criterion for the diagnosis of inflammatory HCA [34]. All 29

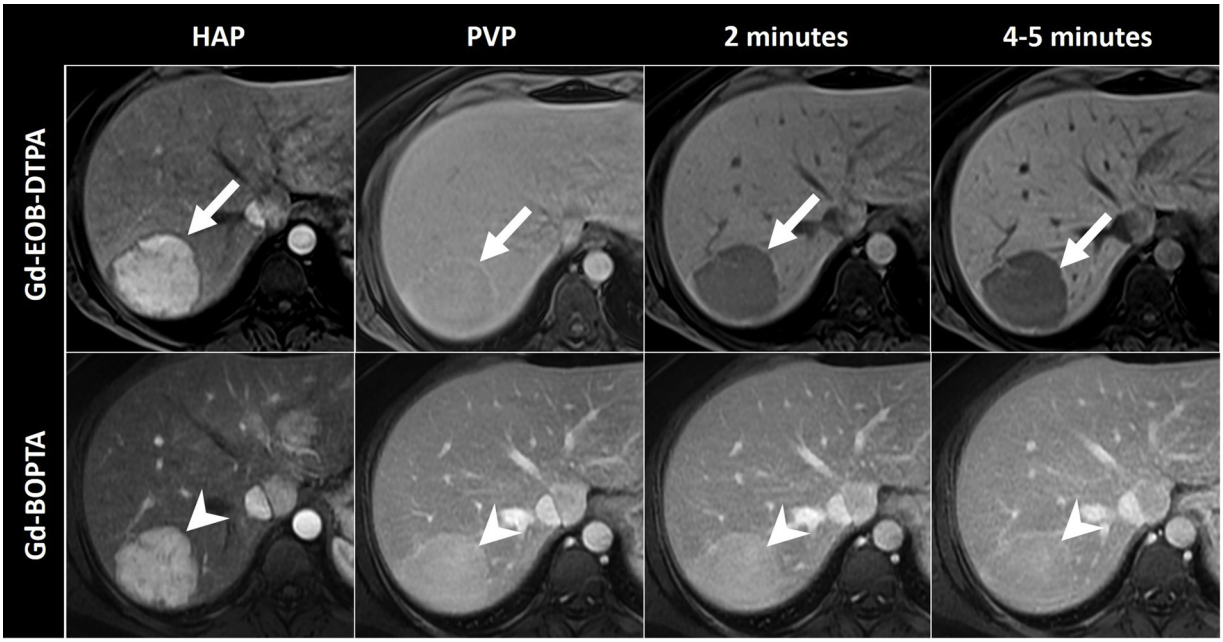

Fig. 3. 32-year-old female with HCA, inflammatory subtype, on axial 3D GRE MR images obtained after IV injection of Gd-EOB-DPTA (upper row) and Gd-BOPTA (lower row). On Gd-EOB-DTPA enhanced MRI the lesion (*arrows* on upper row) shows marked APHE on HAP image, isointensity on PVP, hypointensity on 2 min and 4–5 minutes phase images. On Gd-BOPTA enhanced MRI the lesion (*arrowheads* on lower row) demonstrates marked APHE on HAP image and persistent enhancement on PVP, 2 and 4–5 minutes phase images. Note the pseudocapsule on the Gd-EOB-DTPA enhanced study showing hypointensity on HAP image and progressive retention of contrast on PVP, 2 and 4–5 minutes phase images.

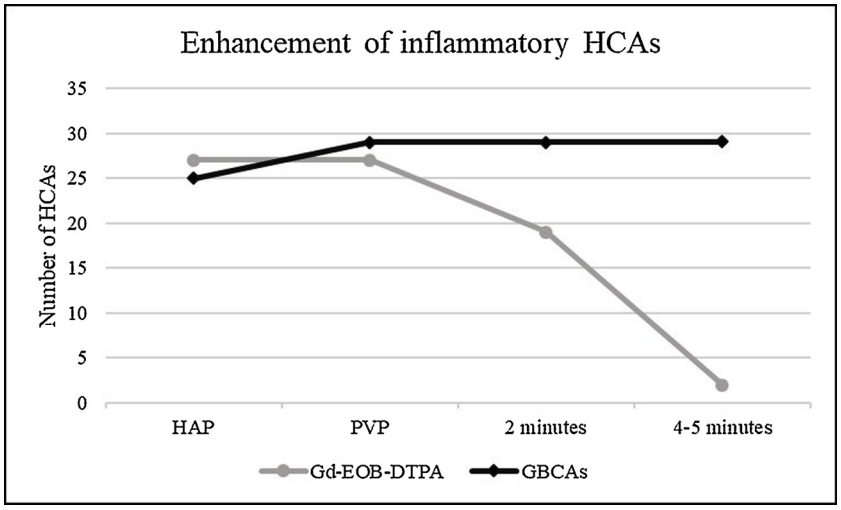

Fig. 4. Graph showing the enhancement of inflammatory HCAs on multiphasic MR imaging after injection of Gd-EOB-DTPA or other GBCAs. HCAs imaged with Gd-EOB-DTPA (*gray line*) show progressive hypointensity on PVP, 2 min and 4–5 minutes phases. HCAs imaged with other GBCAs (*black line*) show persistent enhancement on PVP, 2 min and 4–5 minutes phases.

inflammatory HCAs in our cohort showed persistent enhancement during the PVP, 2 min and 4–5 minutes images acquired after the administration of an extracellular or mainly extracellular GBCA, while 2/29 (7%), 10/29 (34%) and 27/29 (93%) inflammatory HCAs appeared hypointense respectively on the PVP, 2 min and 4–5 minutes images obtained with Gd-EOB-DTPA. Accordingly, the combination of moderate-to-marked APHE and iso- or hyperintensity on PVP and 2 min images allowed to classify as inflammatory HCA 17/29 (58.6%) lesions using Gd-EOB-DTPA and 25/29 (86.2%) lesions using other GBCAs (P = 0.037). Prior studies investigating HCAs on Gd-EOB-DTPA enhanced MRI reported similar post-contrast appearance [8,17,21]. In those studies, lesion hypointensity was observed in 18–58% of all HCAs and 5–17% of inflammatory HCAs on PVP images [8,17,21] as well as 58–93% of all HCAs and 33–52% of inflammatory HCAs on 3 min phase images [8,17]. These results suggest that when using Gd-EOB-DTPA a diagnosis of inflammatory subtype HCA may be compromised given the lack of contrast retention on PVP and later phases images in up to a third of cases. Indeed, a recent study performed by Ba-Ssalamah et al. [8] reported a sensitivity of 80.9% and specificity of 77.3% for diagnosis of inflammatory HCAs imaged with Gd-EOB-DTPA, which is lower than what previously reported with other GBCAs (sensitivity, 82–87.5%; specificity, 85.2–100%) [10,33].

In our population, 3/35 (9%) of HCAs appeared iso-to-hyperintense on images obtained at 20 min (HBP) following the injection of Gd-EOB-DTPA. Our results are consistent with other series reporting 7–26% of all HCAs and up to 25% of inflammatory HCAs to be iso-to-hyperintense to the background liver on HBP [2,17,21,22] due to the increased expression of organic anion transporting polypeptide 1B1/3 (OATP1B1/3) associated with accumulation of Gd-EOB-DTPA [8,35,36]. Finally, we noted the presence of a pseudocapsule in 37% of HCAs (12 inflammatory and 1 unclassified HCAs) on the Gd-EOB-DTPA enhanced MRI studies. This imaging feature was previously described in 14–62%

of inflammatory HCAs imaged with Gd-EOB-DTPA, and is attributed to the compression of hepatic parenchyma at the periphery of the lesion [8,11]. Interestingly, only one HCA demonstrated pseudocapsule following injection of other GBCA, contrarily to what observed in HCC where the "capsule", composed by a combination of fibrosis and sinusoidal dilatation, is more frequently seen on the MRI studies performed with Gd-BOPTA compared to Gd-EOB-DTPA, likely due to the prolonged extracellular effect of Gd-BOPTA resulting in more extended contrast retention in the fibrotic tissue [13].

Our study has several limitations. The final population was small (n = 35 lesions) due to the strict inclusion criteria, i.e. two MR imaging studies with different contrast agents within one year and at least one pathologically proven HCA. The majority of the HCA were classified as inflammatory (83%) and the final cohort included only two HNF1α-mutated and one β-catenin-mutated HCA. Inflammatory-type HCAs may be more likely to undergo biopsy than HNF1 α-mutated lesions that can be confidently diagnosed detecting intralesional fat on imaging. Moreover, only 57% of the lesions were pathologically proven. We assumed that HCAs with identical imaging presentation were of the same molecular subtypes. The MRI studies were acquired on both 1.5 T and 3 T scanners. Although the field strength may affect the signal intensity of the lesion and hepatic parenchyma on post-contrast T1-weighted images, we expect this confounding factor to play a minor role. Lastly, because at our institution an HBP is not routinely acquired when using Gd-BOPTA, a comparison of the imaging appearance of HCAs on HBP images between Gd-BOPTA and Gd-EOB-DTPA was not possible.

In conclusion, the enhancement pattern of HCA, especially inflammatory subtype, was significantly different after injection of Gd-EOB-DTPA compared to other GBCAs. Lesion hypointensity on the PVP, 2 min and 4–5 minutes images was more frequently noted when using Gd-EOB-DTPA.

Disclosures

Roberto Cannella: not any relevant financial relationships with any commercial interest.

Giuseppe Brancatelli: lecture fees from Bayer.

Balasubramanya Rangaswamy: not any relevant financial relationships with any commercial interest.

Marta I. Minervini: not any relevant financial relationships with any commercial interest.

Amir A. Borhani: consultant for Guebert; book contract from Elsevier/Amirsys.

Alessandro Furlan: book contract from Elsevier/Amirsys.

Funding

This research did not receive any specific grant from funding agencies in the public, commercial, or not-for-profit sectors.

Declaration of Competing Interest

The authors declare that they have no conflict of interests.

Acknowledgments

We thank Prof. Valerie Vilgrain, MD (Hopital Beaujon, Paris) for the inspiring discussion that led to the undertaking of this project.

References

[1] European Association for the Study of the Liver (EASL), EASL Clinical Practice Guidelines on the management of benign liver tumours, J. Hepatol. 65 (2016) 386–398, https://doi.org/10.1016/j.jhep.2016.04.001.

[2] Y. Fang, Y. Guo, W. Li, W. Cai, Y. Zhang, G. Hong, Diagnostic value of gadoxetic acid-enhanced MR imaging to distinguish HCA and its subtype from FNH: a systematic review, Int. J. Med. Sci. 14 (2017) 668–674, https://doi.org/10.7150/ijms.17865.

[3] M.D. McInnes, R.M. Hibbert, J.R. Inácio, N. Schieda, Focal nodular hyperplasia and hepatocellular adenoma: accuracy of gadoxetic acid-enhanced MR imaging–a systematic review, Radiology 277 (2015) 413–423, https://doi.org/10.1148/radiol.2015142986.

[4] P. Bioulac-Sage, S. Rebouissou, C. Thomas, J.F. Blanc, J. Saric, A. Sa Cunha, A. Rullier, G. Cubel, G. Couchy, S. Imbeaud, C. Balabaud, J. Zucman-Rossi, Hepatocellular adenoma subtype classification using molecular markers and immunohistochemistry, Hepatology 46 (2007) 740–748, https://doi.org/10.1002/hep.21743.

[5] J. Zucman-Rossi, E. Jeannot, J.T. Nhieu, J.Y. Scoazec, C. Guettier, S. Rebouissou, Y. Bacq, E. Leteurtre, V. Paradis, S. Michalak, D. Wendum, L. Chiche, M. Fabre, L. Mellottee, C. Laurent, C. Partensky, D. Castaing, E.S. Zafrani, P. Laurent-Puig, C. Balabaud, P. Bioulac-Sage, Genotype-phenotype correlation in hepatocellular adenoma: new classification and relationship with HCC, Hepatology 43 (2006) 515–524, https://doi.org/10.1002/hep.21068.

[6] S.M. van Aalten, R.A. de Man, J.N. IJzermans, T. Terkivatan, Systematic review of haemorrhage and rupture of hepatocellular adenomas, Br. J. Surg. 99 (2012) 911–916, https://doi.org/10.1002/bjs.8762.

[7] J.C. Nault, G. Couchy, C. Balabaud, G. Morcrette, S. Caruso, J.F. Blanc, Y. Bacq, J. Calderaro, V. Paradis, J. Ramos, J.Y. Scoazec, V. Gnemmi, N. Sturm, C. Guettier, M. Fabre, E. Savier, L. Chiche, P. Labrune, J. Selves, D. Wendum, C. Pilati, A. Laurent, A. De Muret, B. Le Bail, S. Rebouissou, S. Imbeaud, GENTHEP Investigators, P. Bioulac-Sage, E. Letouzé, J. Zucman-Rossi, Molecular classification of hepatocellular adenoma associates with risk factors, bleeding, and malignant transformation, Gastroenterology 152 (2017) 880–894, https://doi.org/10.1053/j.gastro.2016.11.042 e6.

[8] A. Ba-Ssalamah, C. Antunes, D. Feier, N. Bastati, J.C. Hodge, J. Stift, M.A. Cipriano, F. Wrba, M. Trauner, C.J. Herold, F. Caseiro-Alves, Morphologic and molecular features of hepatocellular adenoma with gadoxetic acid-enhanced MR imaging, Radiology 277 (2015) 104–113, https://doi.org/10.1148/radiol.2015142366.

[9] S.M. van Aalten, M.G. Thomeer, T. Terkivatan, R.S. Dwarkasing, J. Verheij, R.A. de Man, J.N. Ijzermans, Hepatocellular adenomas: correlation of MR imaging findings with pathologic subtype classification, Radiology 261 (2011) 172–181, https://doi.org/10.1148/radiol.11110023.

[10] M. Ronot, S. Bahrami, J. Calderaro, D.C. Valla, P. Bedossa, J. Belghiti, V. Vilgrain, V. Paradis, Hepatocellular adenomas: accuracy of magnetic resonance imaging and liver biopsy in subtype classification, Hepatology 53 (2011) 1182–1191, https://doi.org/10.1002/hep.24147.

[11] J.R. Tse, B.V. Naini, D.S. Lu, S.S. Raman, Qualitative and quantitative gadoxetic acid-enhanced MR imaging helps subtype hepatocellular adenomas, Radiology 279 (2016) 118–127, https://doi.org/10.1148/radiol.2015142449.

[12] T. Tirkes, P. Mehta, A.M. Aisen, C. Lall, F. Akisik, Comparison of dynamic phase enhancement of hepatocellular carcinoma using gadoxetate disodium vs gadobenate dimeglumine, J. Comput. Assist. Tomogr. 39 (2015) 479–482, https://doi.org/10.1097/RCT.0000000000000234.

[13] M. Dioguardi Burgio, D. Picone, G. Cabibbo, M. Midiri, R. Lagalla, G. Brancatelli, MR-imaging features of hepatocellular carcinoma capsule appearance in cirrhotic liver: comparison of gadoxetic acid and gadobenate dimeglumine, Abdom. Radiol. (NY) 41 (2016) 1546–1554, https://doi.org/10.1007/s00261-016-0726-7.

[14] Y. Park, S.H. Kim, S.H. Kim, Y.H. Jeon, J. Lee, M.J. Kim, D. Choi, W.J. Lee, H. Kim, J.H. Koo, H.K. Lim, Gadoxetic acid (Gd-EOB-DTPA)-enhanced MRI versus gadobenate dimeglumine (Gd-BOPTA)-enhanced MRI for preoperatively detecting hepatocellular carcinoma: an initial experience, Korean J. Radiol. 11 (2010) 433–440, https://doi.org/10.3348/kjr.2010.11.4.433.

[15] R.T. Gupta, D. Marin, D.T. Boll, D.B. Husarik, D.E. Davis, S. Feuerlein, E.M. Merkle, Hepatic hemangiomas: difference in enhancement pattern on 3T MR imaging with gadobenate dimeglumine versus gadoxetate disodium, Eur. J. Radiol. 81 (2012) 2457–2462, https://doi.org/10.1016/j.ejrad.2011.10.014.

[16] R.T. Gupta, C.M. Iseman, J.R. Leyendecker, I. Shyknevsky, E.M. Merkle, B. Taouli, Diagnosis of focal nodular hyperplasia with MRI: multicenter retrospective study comparing gadobenate dimeglumine to gadoxetate disodium, AJR Am. J. Roentgenol. 199 (2012) 35–43, https://doi.org/10.2214/AJR.11.7757.

[17] L. Grazioli, M.P. Bondioni, H. Haradome, U. Motosugi, R. Tinti, B. Frittoli, S. Gambarini, F. Donato, S. Colagrande, Hepatocellular adenoma and focal nodular hyperplasia: value of gadoxetic acid-enhanced MR imaging in differential diagnosis, Radiology 262 (2012) 520–529, https://doi.org/10.1148/radiol.11101742.

[18] L. Grazioli, G. Morana, M.A. Kirchin, G. Schneider, Accurate differentiation of focal nodular hyperplasia from hepatic adenoma at gadobenate dimeglumine-enhanced MR imaging: prospective study, Radiology 236 (2005) 166–177, https://doi.org/10.1148/radiol.2361040338.

[19] M. Roux, F. Pigneur, L. Baranes, J. Calderaro, M. Chiaradia, T. Decaens, S. Kastahian, A. Charles-Nelson, L. Tselikas, C. Costentin, A. Laurent, D. Azoulay, A. Mallat, A. Rahmouni, A. Luciani, Differentiating focal nodular hyperplasia from hepatocellular adenoma: Is hepatobiliary phase MRI (HBP-MRI) using linear gadolinium chelates always useful? Abdom. Radiol. (NY) 43 (2018) 1670–1681, https://doi.org/10.1007/s00261-017-1377-z.

[20] H. Wang, C. Yang, S. Rao, Y. Ji, J. Han, R. Sheng, M. Zeng, MR imaging of hepatocellular adenomas on genotype-phenotype classification: a report from China, Eur. J. Radiol. 100 (2018) 135–141, https://doi.org/10.1016/j.ejrad.2018.01.023.

[21] C. Grieser, I.G. Steffen, I.B. Kramme, H. Bläker, E. Kilic, C.M. Perez Fernandez, D. Seehofer, E. Schott, B. Hamm, T. Denecke, Gadoxetic acid enhanced MRI for differentiation of FNH and HCA: a single centre experience, Eur. Radiol. 24 (2014) 1339–1348, https://doi.org/10.1007/s00330-014-3144-7.

[22] J.F. Glockner, C.U. Lee, T. Mounajjed, Inflammatory hepatic adenomas: characterization with hepatobiliary MRI contrast agents, Magn. Reson. Imaging 47 (2018) 103–110, https://doi.org/10.1016/j.mri.2017.12.006.
[23] T. Denecke, I.G. Steffen, S. Agarwal, D. Seehofer, T. Kröncke, E.L. Hänninen, I.B. Kramme, P. Neuhaus, S. Saini, B. Hamm, C. Grieser, Appearance of hepatocellular adenomas on gadoxetic acid-enhanced MRI, Eur. Radiol. 22 (2012) 1769–1775, https://doi.org/10.1007/s00330-012-2422-5.
[24] M.G. Thomeer, F.E. Willemssen, K.K. Biermann, H. El Addouli, R.A. de Man, J.N. Ijzermans, R.S. Dwarkasing, MRI features of inflammatory hepatocellular adenomas on hepatocyte phase imaging with liver-specific contrast agents, J. Magn. Reson. Imaging 39 (2014) 1259–1264, https://doi.org/10.1002/jmri.24281.
[25] I.J.S.M.L. Vanhooymissen, M.G. Thomeer, L.M.M. Braun, B. Gest, S. van Koeverden, F.E. Willemssen, M. Hunink, R.A. De Man, J.N. Ijzermans, R.S. Dwarkasing, Intrapatient comparison of the hepatobiliary phase of Gd-BOPTA and Gd-EOB-DTPA in the differentiation of hepatocellular adenoma from focal nodular hyperplasia, J Magn Reson Imaging 49 (3) (2019) 700–710, https://doi.org/10.1002/jmri.26227.
[26] T.J. Vogl, S. Kümmel, R. Hammerstingl, M. Schellenbeck, G. Schumacher, T. Balzer, W. Schwarz, P.K. Müller, W.O. Bechstein, M.G. Mack, O. Söllner, R. Felix, Liver tumors: comparison of MR imaging with Gd-EOB-DTPA and Gd-DTPA, Radiology 200 (1996) 59–67, https://doi.org/10.1148/radiology.200.1.8657946.
[27] L. Arrivé, J.F. Fléjou, V. Vilgrain, J. Belghiti, D. Najmark, M. Zins, Y. Menu, J.M. Tubiana, H. Nahum, Hepatic adenoma: MR findings in 51 pathologically proved lesions, Radiology 193 (1994) 507–512, https://doi.org/10.1148/radiology.193.2.7972769.
[28] B. Hamm, T. Staks, A. Mühler, M. Bollow, M. Taupitz, T. Frenzel, K.J. Wolf, H.J. Weinmann, L. Lange, Phase I clinical evaluation of Gd-EOB-DTPA as a hepatobiliary MR contrast agent: safety, pharmacokinetics, and MR imaging, Radiology 195 (1995) 785–792, https://doi.org/10.1148/radiology.195.3.7754011.
[29] S. Dokmak, V. Paradis, V. Vilgrain, A. Sauvanet, O. Farges, D. Valla, P. Bedossa, J. Belghiti, A single-center surgical experience of 122 patients with single and multiple hepatocellular adenomas, Gastroenterology 137 (2009) 1698–1705, https://doi.org/10.1053/j.gastro.2009.07.061.
[30] J.H. Stoot, R.J. Coelen, M.C. De Jong, C.H. Dejong, Malignant transformation of hepatocellular adenomas into hepatocellular carcinomas: a systematic review including more than 1600 adenoma cases, HPB (Oxford) 12 (2010) 509–522, https://doi.org/10.1111/j.1477-2574.2010.00222.x.
[31] S.S. Liau, M.S. Qureshi, R. Praseedom, E. Huguet, Molecular pathogenesis of hepatic adenomas and its implications for surgical management, J. Gastrointest. Surg. 17 (2013) 1869–1882, https://doi.org/10.1007/s11605-013-2274-6.
[32] E.P. Scali, T. Walshe, H.A. Tiwari, A.C. Harris, S.D. Chang, A pictorial review of hepatobiliary magnetic resonance imaging with hepatocyte-specific contrast agents: uses, findings, and pitfalls of gadoxetate disodium and gadobenate dimeglumine, Can. Assoc. Radiol. J. 68 (2017) 293–307, https://doi.org/10.1016/j.carj.2016.10.008.
[33] H. Laumonier, P. Bioulac-Sage, C. Laurent, J. Zucman-Rossi, C. Balabaud, H. Trillaud, Hepatocellular adenomas: magnetic resonance imaging features as a function of molecular pathological classification, Hepatology 48 (2008) 808–818, https://doi.org/10.1002/hep.22417.
[34] P. Attal, V. Vilgrain, G. Brancatelli, V. Paradis, B. Terris, J. Belghiti, B. Taouli, Y. Menu, Telangiectatic focal nodular hyperplasia: US, CT, and MR imaging findings with histopathologic correlation in 13 cases, Radiology 228 (2003) 465–472, https://doi.org/10.1148/radiol.2282020040.
[35] N. Yoneda, O. Matsui, A. Kitao, K. Kozaka, S. Kobayashi, M. Sasaki, K. Yoshida, D. Inoue, T. Minami, T. Gabata, Benign hepatocellular nodules: hepatobiliary phase of gadoxetic acid-enhanced MR imaging based on molecular background, Radiographics 36 (2016) 2010–2027, https://doi.org/10.1148/rg.2016160037.
[36] N. Yoneda, O. Matsui, A. Kitao, K. Kozaka, T. Gabata, M. Sasaki, Y. Nakanuma, K. Murata, T. Tani, Beta-catenin-activated hepatocellular adenoma showing hyperintensity on hepatobiliary-phase gadoxetic-enhanced magnetic resonance imaging and overexpression of OATP8, J. Radiol. 30 (2012) 777–782, https://doi.org/10.1007/s11604-012-0115-2.